Magnetic Properties of Nanodispersed Ferrite Powders with Cryochemical Prehistory

K. A. Mozul'[a], L. P. Ol'khovik[a], E. V. Shurinova[a], S. V. Blazhevich[b], T. G. Kuz'micheva[b], S. V. Chernikov[b], and A. S. Kamzin[c, *]

[a] *Kazarin Kharkov National University, pl. Svobody 4, Kharkov, 61077 Ukraine*

[b] *Centre of Nanostructural Materials and Nanotechnologies, Belgorod State University, ul. Koroleva 2a, Belgorod, 308034 Russia*

[c] *Ioffe Physical-Technical Institute, Russian Academy of Sciences, Politekhnicheskaya ul. 26, St. Petersburg, 194021 Russia*

Abstract—Calcium hexagonal ferrite in the form of a system of nanocrystals has been synthesizes using elements of cryochemical technology for the first time. The obtained ensemble of particles corresponds to the model Stoner–Wohlfarth system according to the following characteristics: the phase composition, the shape of the basic magnetization curve, and the coercive force. The temperature dependences of the magnetization in the range 300–700 K at fixed values of the magnetic field indicate the presence of a transition to the superparamagnetic (SPM) state. The boundary temperatures $T_{BH}^{(1)}$ and T_{BH}^{2} of the range of the SPM transition have been determined, and the role of the external magnetic field, which stimulates the transition in this process in accordance with the theory, has been confirmed.

1. INTRODUCTION

In the last decade, methods for obtaining and studying the fundamental properties of nanodispersed magnetic materials have been intensively developed. Of special interest for creation of new magnetic materials for innovative medicobiological technologies is the class of hexagonal ferrites. The interest in these ferrites is associated with the possibility of performing the effective control over the properties of hexagonal ferrites by introducing dia- and paramagnetic ions, as well as with the special features of the superparamagnetic (SPM) state, which is inherent in ultrasmall particles.

The ferrite powder synthesized in this work was intended for development of a new class of biologically compatible composite materials on the basis of calcium, in which nanocrystalline particles of hexagonal ferrite $Ca_{0.5}Ba_{0.5}Fe_{12}O_{19}$ were used for the first time as the magnetic component [1–5]. This composition has the highest degree of structural similarity with the mineral components of bone and bone implants on the basis of hydroxyapatite $Ca_{0.5}(PO_4)_3OH$. However, when obtaining calcium hexaferrite, certain difficulties arise in matching a number of technological and output functional parameters (chemical homogeneity of initial materials, the temperature and duration of synthesis, the single-phase composition of the finished product, the shape and diameter of particles, the absence of conglomerates in powder, the saturation magnetization, the coercive force, and the magnetic state).

The objective of the present study was to develop a method for synthesis of nanocrystals from calcium hexagonal ferrite using elements of cryochemical technology and to investigate the specific size effect caused by the transition of particles of the system from the magnetostable state to the SPM state.

2. EXPERIMENTAL TECHNIQUES

2.1. Method for Preparing Highly Dispersed Powders of Calcium Hexagonal Ferrite

One of the prior conditions for the synthesis of nanodispersed ferrite particles of the composition $Ca_{0.5}Ba_{0.5}Fe_{12}O_{19}$, the preparation of which runs into difficulties caused by the critically small radius of calcium ions, is the high chemical homogeneity of the initial ferrite-forming mixture. Therefore, for preparing the initial multicomponent salt mixture, the most effective cryochemical technology was used [6]. In the framework of the employed cryochemical technology, the mixed stoichiometric solution of the compatible salts $Ca(CH_3COO)_2$ (reagent grade), $Ba(NO_3)_2$ (reagent grade), and $Fe(CHOO)_3$ (chemically pure) was dispersed by means of a pneumatic nozzle to liquid nitrogen. Subsequent sublimation drying (dehydration) of formed cryogranules of micrometer sizes was performed in a sublimer on pans of stainless steel,

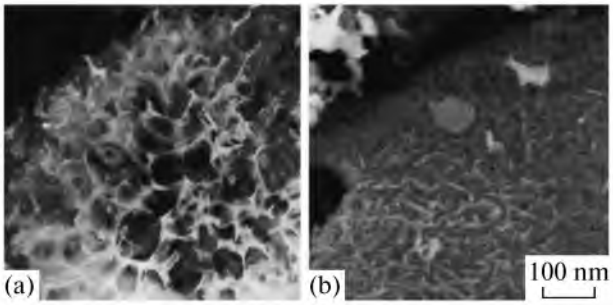

Fig. 1. Electron microscopy images of the salt framework of (a) the cryogranule and (b) self-organized $Ca_{0.5}Ba_{0.5}Fe_{12}O_{19}$ nanocrystals in the format of the cryogranule.

which were placed on trays of the sublimer, preliminarily cooled to ~–40°C. The sublimation process was continuous and lasted for 23–25 h at T ~–50°C and $P = 2.66–13.30$ Pa. The dehydrated salt mixture in the form of isolated frameworks is shown in Fig. 1a.

The technological operation preceding ferritization consisted in thermal decomposition of the components of the salt mixture. The thermolysis temperature of the mixture of the initial components must be not lower than the thermolysis temperature of each component. Of the above-mentioned transitions in the acetate series, the transition $Ca(CH_3COO)_2 \longrightarrow CaO$ has the highest temperature. The stage-wise thermal decomposition of calcium acetate to the oxide proceeds by the scheme

$$Ca(CH_3COO)_2 \xrightarrow[160°C]{} Ca_2C_2O_4 \xrightarrow[200°C]{} CaCO_3 \xrightarrow[825°C]{} CaO. \quad (1)$$

Since, in the case of the macroscopic analogue of $Ca_{0.5}Ba_{0.5}Fe_{12}O_{19}$, complete ferritization is provided by the temperature of 1270°C [7], i.e., higher than for hexaferrite $BaFe_{12}O_{19}$ (1150°C), in the case of a highly dispersed system of particles, the ferritization was performed, by analogy, at a higher temperature, namely, in the region of 900–1000°C, whereas ferritization of nanodispersed powder of barium ferrite is usually performed at 800°C. Decomposition of the products of cryogenic synthesis and subsequent ferritization were performed in alundum cups with a bulk load layer (4–7 mm), placed to a high-temperature muffle heater.

2.2. Methods for Measuring the Parameters of Powder Samples

Different methods were used for systematic analysis of the quality of the obtained powder sample. The phase composition and structure of the synthesized materials were performed by a STOE (DTOE&Cie GmbH, Germany) CoK_α radiation diffractometer, Mössbauer spectroscopy, and electron microscopy.

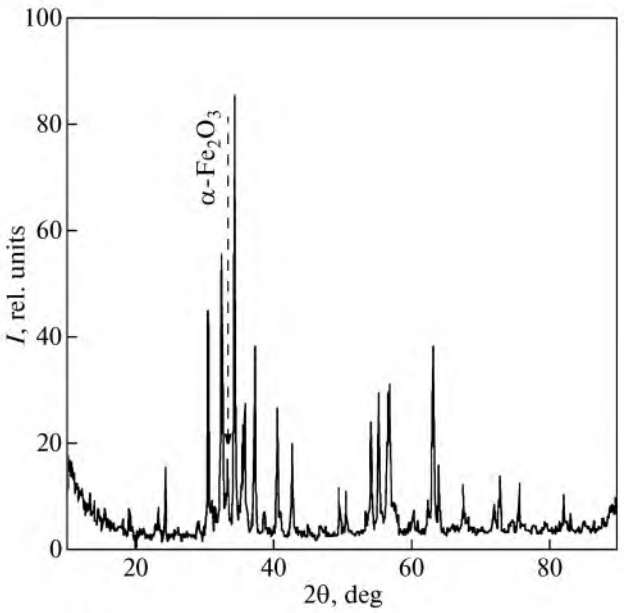

Fig. 2. X-ray diffraction pattern of the powder of hexagonal ferrite $Ca_{0.5}Ba_{0.5}Fe_{12}O_{19}$ synthesized at 900°C.

The X-ray diffraction patterns were interpreted by means of the PDF-2JCPDS (Joint Committee on Power Diffraction Standards) data base. Mössbauer spectra were obtained in the geometry of transmission of gamma radiation from a Co^{57} gamma-quantum source in a rhodium matrix moving with a triangular acceleration. The microstructure and elemental analysis were performed by means of a Selmi PEM-125K (Selmi, Ukraine) electron microscope. The magnetic characteristics (parameters of the hysteresis loop, saturation magnetization, residual magnetization, and coercive force) were measured by a vibration magnetometer.

3. RESULTS OF STUDYING THE PHASE COMPOSITION OF SYNTHESIZED FERRITE POWDERS

The electron microscopy image shown in Fig. 1b illustrates the process of formation of plate-like crystals in the format of a cryogranule. We can see rather a dense self-organized arrangement of particles oriented with respect to each other mainly by the basis planes. More rarely, single plate-like particles with a distinct hexagonal form occur on the microreactor surface (the salt framework of a cryogranule). The size of individual particles corresponds to the nanometer scale.

The phase structure of synthesized powder was analyzed by means of an x-ray diffractometer. An example of x-ray diffraction pattern of ferrite powder is shown in Fig. 2. The data obtained from interpretation of x-ray diffraction patterns using the PDF-2JCPDS data base are presented in table. In addition to the main phase of hexagonal ferrite, there is an

Results of the interpretation of the diffraction patterns of the $Ca_{0.5}Ba_{0.5}Fe_{12}O_{19}$ powder synthesized at 900°C

No.	*I*, rel. units	2θ, deg	θ, deg	sinθ	*d*, Å	*hkl*	*a*, Å	*c*, Å
1	5.9	23.27	11.635	0.20158	3.820	006	–	22.919
2	65.7	30.44	15.220	0.2624	2.935	110	5.869	–
3	10.33	31.37	15.685	0.27021	2.850	008	–	22.797
4	89.7	32.30	16.150	0.27802	2.770	107	–	–
5	7.0	33.20	16.600	0.28555	2.697	112	–	–
6	100.0	34.29	17.145	0.29465	2.613	114	–	–
7	34.0	35.47	17.735	0.30447	2.529	200	5.841	–
8	56.7	37.15	18.575	0.31839	2.418	203	–	–
9	3.7	39.30	19.650	0.33611	2.291	109	–	–
10	32.96	40.44	20.220	0.34546	2.229	205	–	–
11	25.19	42.57	21.285	0.36283	2.122	206	–	–
12	5.9	50.36	25.180	0.42526	1.811	209	–	–
13	38.7	55.20	27.600	0.46308	1.663	127	–	–
14	42.04	56.60	28.300	0.47387	1.625	304	–	–
15	50.67	63.07	31.535	0.52278	1.473	220	5.892	–
16	8.8	67.42	33.710	0.55474	1.388	2.0.14	–	–
17	11.8	72.77	36.385	0.59295	1.299	317	–	–

admixture of α-F_2O_3, whose content, according to the data of x-ray phase analysis, does not exceed 5%. The arrow in the diffraction pattern (Fig. 2) marks the reflex of the maximum intensity, corresponding to the admixture phase. Calculations of the parameters of the crystal lattice of calcium hexaferrite have shown that the lattice parameter *a* remains practically equal to the basis composition of $BaFe_{12}O_{19}$ [8], and the observed decrease in the lattice parameter *c* indirectly confirms that Ca^{2+} ions have entered the crystal structure of ferrite.

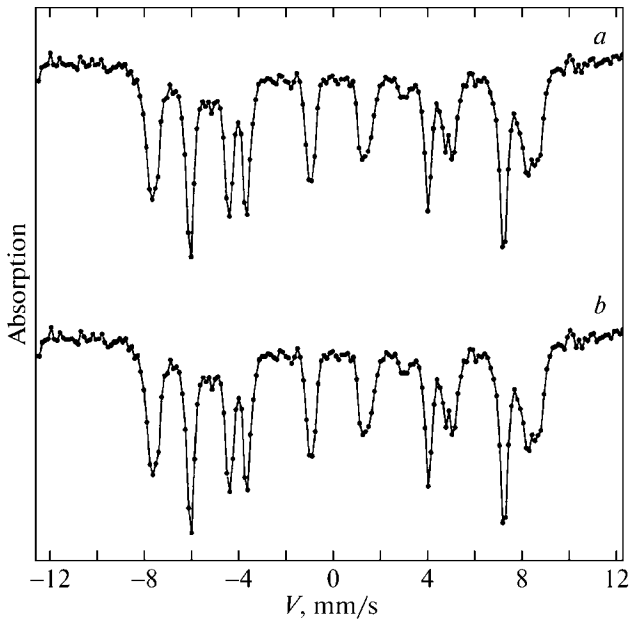

Fig. 3. Mössbauer spectra of the system of $Ca_{0.5}Ba_{0.5}Fe_{12}O_{19}$ nanocrystals obtained at (*a*) 77 and (*b*) 300 K.

The Mössbauer analysis confirms that the synthesized $Ca_{0.5}Ba_{0.5}Fe_{12}O_{19}$ nanocrystals obtained at room temperature can be assigned to the hexagonal ferrite of structural type *M*. Figure 3 presents experimental Mössbauer spectra of nanocrystalline $Ca_{0.5}Ba_{0.5}Fe_{12}O_{19}$ obtained at room temperature and at the temperature of liquid nitrogen. Mathematical processing of the experimental Mössbauer spectra was performed by means of the program described in [9]. The spectrum consists of a set of Zeeman sextets emerging due to the absorption of gamma-quanta by isotopes (Fe^{57}) of iron ions of various crystallographic positions. The line intensity ratios (Fig. 3) in the sextets are 3:2:1:1:2:3, which is typical for powder samples. The parameters of hyperfine interactions (HFI), namely: the effective magnetic fields, quadrupole splittings, and isomeric chemical shifts, calculated from the spectrum of $Ca_{0.5}Ba_{0.5}Fe_{12}O_{19}$ (Fig. 3), are close to the HFI parameters of hexagonal ferrites of type *M* [10]. The Mössbauer spectra have no additional lines indicating the presence of an irrelevant phase and no lines in the region of zero velocity, which belongs to the paramagnetic or HFI phase

4. MAGNETIC PROPERTIES OF SYNTHESIZED FERRITE POWDERS

For estimating the quality of the obtained powder as a magnetic material, it was sufficient to establish the form of the main magnetization curve and determine the coercive force at 300 K. The measurements were performed on a thermally demagnetized squeezed (the packing factor $p \sim 0.4$) powder sample with disorderly oriented particle in the fields up to 20 kOe.

The shape of the obtained magnetization curve $\sigma(H)$ and the ultimately small coercive force determined from the hysteresis loop ($H_C = 2250$ Oe) (curve *1* in Fig. 4) have been an unexpected result for cryogenic technology, which does not allow this powder to be classified as a model system [11, 12]. The comparative analysis of the coercive force for $BaFe_{12}O_{19}$ powders of different dispersiveness leads to certain assumption concerning this result. Taking into account that the high-temperature synthesis of ferrite powder did not employ the flux component in the process of ferritization and nanocrystal formation, we may assume that partial conglomeration took place. Therefore, the technological chain described above was complemented with grinding the finished product in water medium. As is evident from the electron microscopy image presented in Fig. 4, this procedure has not led to changing the dispersiveness of the powder. The size of individual particles still belongs to the nanometer range and comprises 10–60 nm.

In order to confirm or refute the assumption of partial conglomeration of particles, after correcting the technology, attestation of the powder was performed again. The test consisted in measuring the main magnetization curve and the limiting hysteresis loop at 300 K. The results are shown in Fig. 4 (curve *2*). As is evident, the main magnetization curve agrees with the theoretical Stoner–Wohlfarth (SW) curve [11]. The small deviation (in the form of a bulge) from linearity of the initial section ($H = 0$–3500 Oe) indicates the presence of a small amount of microcrystalline particles in the powder. The value of the coercive force $H_C = 5300$ Oe agrees with that for the model SW system of $BaFe_{12}O_{19}$ nanocrystals [11].

Thus, the correction of the technology of obtaining calcium ferrite powder made it possible to restore the magnetic properties inherent in a system of single-domain particles.

5. INVESTIGATION OF THE MAGNETIC STATE OF A SYSTEM OF $Ca_{0.5}Ba_{0.5}Fe_{12}O_{19}$ NANOCRYSTALS IN THE TEMPERATURE RANGE 300 K–T_C

By estimating the critical superparamagnetic volume $V_{SO}(H = 0)$ and comparing it with the real average volume $\langle V \rangle$ of the particle size distribution, the possibility to realize the SPM state of particles of the system under study has been found out. The critical volume at

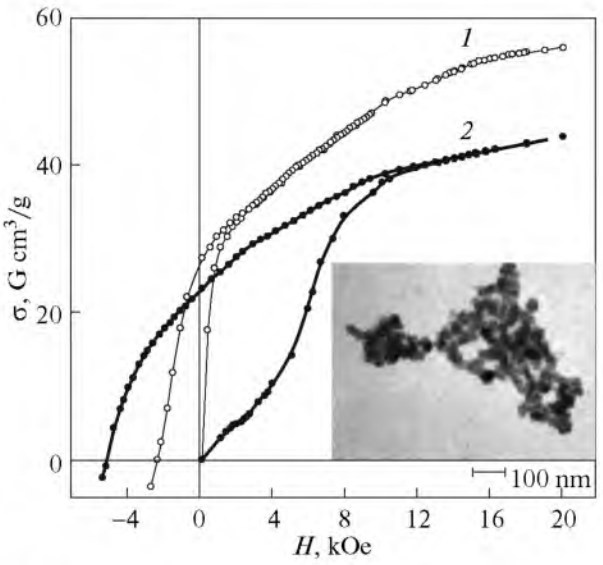

Fig. 4. Basic magnetization curves and fragments of limiting hysteresis loops of a powder sample of the calcium-containing hexaferrite obtained at 300 K (*1*) before and (*2*) after grinding. The inset shows the electron microscopy image of the ground powder.

which the particle passes from the magnetostable (MS) state to the SPM state is determined from the equality between the energy of magnetic anisotropy of a particle and thermal energy:

$$KV_{SO} = 25kT \quad \text{or} \quad H_a I_S V_{SO} = 50kT. \qquad (2)$$

Here, K is the effective magnetic anisotropy constant, I_S is the magnetization in the anisotropy field of the macroscopic analogue, and $H_a = \langle H_a \rangle$, where $\langle H_a \rangle$ is the mean of the anisotropy field distribution of particles. The critical volume for $T = 300$ K is V_{SO} (300 K) $= 1 \times 10^{-18}$ cm^3, which is less than the real volume of a particle, which, for the diameter $\langle d \rangle = 35$ nm, is $\langle V \rangle = 7 \times 10^{-18}$ cm^3. Thus, at room temperature, the major part of particles of the system under study is in the MS state. This fact is confirmed by the results of Mössbauer studies, which enable one to obtain information on the magnetic state of the nanodispersed system. As is evident from Fig. 3, the Mössbauer spectra obtained at 77 and 300 K consist of the Zeeman sextets and, in the vicinity of zero velocities, no lines belonging to paramagnetic doublets indicating the loss of the magnetic stability of nanoparticles under study and the emergence of the SPM state are observed. Hence, in the considered temperature range (77–300 K), the SPM state in a system of particles of highly anisotropic calcium hexagonal ferrite are not realized.

With an increase in temperature, the critical volume substantially increases (V_{SO} (600 K) $= 7 \times 10^{-18}$ cm^3, hence the probability of transition of particles into the SPM state increases too. Nevertheless, the average

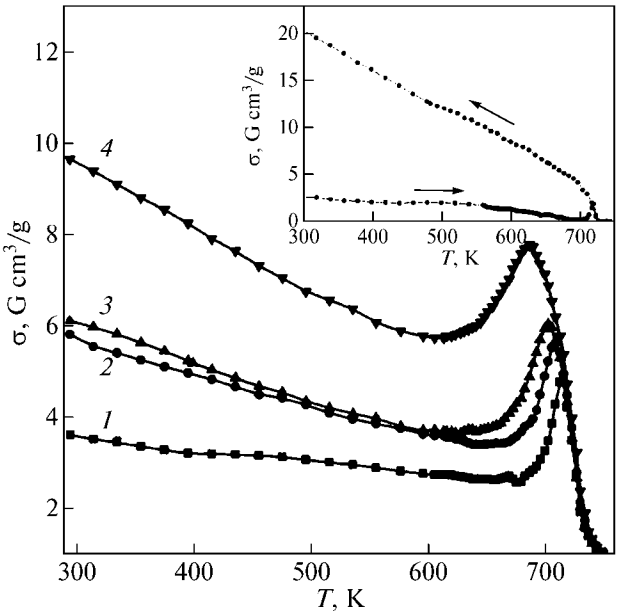

Fig. 5. Temperature dependences of the specific magnetization at fixed values of the external magnetic field ($H \ll H_a$) H = (*1*) 1.0, (*2*) 1.5, (*3*) 2.0, and (*4*) 3.0 kOe. The inset shows the temperature dependence of the magnetization in the external magnetic field H = 5 kOe during heating and cooling.

volume of particles still exceeds the critical volume. For realization of the transition, stimulating action of the external magnetic field is necessary, because, in the presence of the field, the critical volume increases according to the formula $V_{SH} = V_{SO}/(1 - H/H_\alpha)^2$.

According to the theoretical model developed in [13], the transition of the system of single-domain particles is indicated by the presence of a maximum in the temperature dependence of magnetization. The character of the experimental temperature dependences of the specific magnetization σ for a system of $Ca_{0.5}Ba_{0.5}Fe_{12}O_{19}$ nanocrystals for the values of the magnetic field of 1.0, 1.5, 2.0, and 3.0 kOe (Fig. 5) fully agrees with the theoretic results for small fields ($H \ll H_a$). The temperature at which the maximum in the curve $\sigma(T)$ is observed is introduced as the blocking temperature $T_{BH}^{(2)}$. As expected, with an increase in the field, $T_{BH}^{(2)}$ is displaced towards lower temperatures with simultaneous smearing of the observed anomaly.

For a real system in which particles are distributed with respect to their volume and effective magnetic anisotropy fields, the SPM transition is realized in a certain temperature range $T_{BH}^{(1)} - T_{BH}^{(2)}$, where $T_{BH}^{(1)}$ corresponds to the temperature from which the monotonic decrease in the magnetization is disturbed and replaced by subsequent rather a sharp increase.

The observed anomaly, whose form resembles the Hopkinson effect, is associated with the deblocking caused by thermal energy and the energy of external magnetic field of the magnetic moments of nanocrystals with $V = V_{SH}$, blocked earlier by the magnetic anisotropy energy.

Another typical feature of the magnetic state transitions MS ⟶ SPM (heating in the field) and SPM ⟶ MS (cooling in the field) is the mismatch between the forward ($\sigma(T)$) and reverse ($\sigma^*(T)$) dependences under study. This fact is illustrated by Fig. 5 (inset). It is readily seen that the dependence $\sigma^*(T)$ for the case of H = 0.5 kOe is not anomalous and its value at 300 K exceeds σ 7-fold. According to theoretical estimates of [13], in the limiting case when $H \longrightarrow 0$, the effect of irreversibility of $\sigma(T)$ must increase up to 26. The experimental data obtained for a system of $BaFe_{12}O_{19}$ nanocrystals in a field of 0.25 kOe [14] are close to the theoretical value.

6. CONCLUSIONS

For the first time, using elements of cryochemical technology, a system of nanocrystals of calcium hexagonal ferrite has been synthesized for (due to improved biological compatibility of chemical composition) further approbation as magnetic nanoagents for medico-biological purposes. Attestation of the experimental powder sample with respect to a number of parameters has been performed. The initially observed inconformity of the attestation parameters to a system of single-domain particles has been removed by additional grinding of the powder at the final stage of the technological process. The repeated attestation has confirmed the conformity of the powder to the model system of small Stoner–Wohlfarth particles.

In experimental studied of the temperature dependences of magnetization in small fields ($H \ll H_a$), a dimensional effect has been found in the high-temperature region, which is associated with changes in the magnetic states of particles with volumes close to critical. From the viewpoint of prospects to use particles of this ferrite as magnetic nanoagents in medical technologies, it is of interest to find more exactly the optimal conditions for formation of the SPM state of particle directly in the therapeutical temperature region.

ACKNOWLEDGMENTS

This study was supported by the State Foundation for Basic Research of the Ministry of Science and Education of Ukraine within the framework of the Russian–Ukrainian International Project for 2009–2010 (project no. F 28.7/014), the Russian Foundation for Basic Research (project no. 09-02-90447-Ukr_f_a), and the Foundation for Basic Research of the Ministry of Science and Education of Ukraine (contract no. F 25/229-2008).

We are grateful to the Center of Collective Use "Diagnostics of the Structure and Properties of Nano-

materials" and the Scientific and Educational Innovation Center "Nanostructured Materials and Nanotechnologies" of the Belgorod State University.

REFERENCES

1. Z. Z. Zyman, M. V. Tkachenko, L. P. Ol'khovik, and N. V. Debukh, in *Proceedings of the International Conference "Functional Materials," Crimea, Ukraine, 2007*, p. 503.
2. Z. Z. Zyman, M. V. Tkachenko, and D. V. Polevodin, J. Mater. Sci.: Mater. Med. **19**, 2819 (2008).
3. Yu. N. Primak and N. Tkachenko, Visn. Khark. Nats. Univ. im. V. N. Kazarina, Ser. Fiz. **821**, 113 (2008).
4. N. V. Tkachenko, L. P. Ol'khovik, and A. S. Kamzin, Phys. Solid State **53** (8), 1588 (2011).
5. N. V. Tkachenko, L. P. Ol'khovik, and A. S. Kamzin, Tech. Phys. Lett. **37** (6), 494 (2011).
6. Yu. D. Tret'yakov, N. N. Oleinikov, and A. P. Mozhaev, *Principles of Cryochemical Technology: A Textbook* (Vysshaya Shkola, Moscow, 1987) [in Russian].
7. H. Yamamoto, T. Kawaguchi, and M. Nagakura, Funtai oyobi Funmatsu Yakin (J. Jpn. Soc. Powder Powder Metall.) **25** (7), 24 (1973).
8. J. Smit and H. P. J. Wijn, *Ferrites* (Wiley, New York, 1959; Inostrannaya Literatura, Moscow, 1962).
9. V. S. Rusakov, Izv. Akad. Nauk, Ser. Fiz. **63** (7), 1389 (1999).
10. A. S. Kamzin, V. L. Rozenbaum, and L. P. Ol'khovik, JETP **84** (4), 788 (1997).
11. E. S. Stoner and E. P. Wohlfarth, IEEE Trans. Magn. **27**, 3469 (1991).
12. Z. V. Golubenko, A. S. Kamzin, L. P. Ol'khovik, M. M. Khvorov, Z. I. Sizova, and V. P. Shabatin, Phys. Solid State. **44** (9), 1698 (2002).
13. H. Pfeiffer and W. Schüppel, J. Magn. Magn. Mater. **30**, 92 (1994).
14. H. Pfeiffer, Phys. Status Solidi A **120**, 233 (1990).